REPORT

ULTRACOLD MOLECULES

Second-scale nuclear spin coherence time of ultracold $^{23}Na^{40}K$ molecules

Jee Woo Park,[1]* Zoe Z. Yan,[1] Huanqian Loh,[1,2] Sebastian A. Will,[1]† Martin W. Zwierlein[1]‡

Coherence, the stability of the relative phase between quantum states, is central to quantum mechanics and its applications. For ultracold dipolar molecules at sub-microkelvin temperatures, internal states with robust coherence are predicted to offer rich prospects for quantum many-body physics and quantum information processing. We report the observation of stable coherence between nuclear spin states of ultracold fermionic sodium-potassium (NaK) molecules in the singlet rovibrational ground state. Ramsey spectroscopy reveals coherence times on the scale of 1 second; this enables high-resolution spectroscopy of the molecular gas. Collisional shifts are shown to be absent down to the 100-millihertz level. This work opens the door to the use of molecules as a versatile quantum memory and for precision measurements on dipolar quantum matter.

Quantum systems with robust coherence have enabled seminal advances in science and technology (*1*), from atomic clocks and precision tests of fundamental laws of nature to the realization of ultracold quantum gases. Ultracold molecules, with their rich internal degrees of freedom, represent an especially attractive platform (*2*, *3*). The electronic, vibrational, rotational, and hyperfine states of a single molecule provide a dense spectral ruler that encompasses the optical-, microwave-, and radio-frequency domains. Precision measurements may be performed in all these spectral regimes and self-consistently compared (*4*, *5*). The crucial prerequisite is having pairs of states with robust coherence. These then enable high-resolution spectroscopy of internal molecular structure, which can be sensitive to physics beyond the Standard Model (*6*). In particular, ultracold molecules with an electric dipole moment open new routes in quantum many-body physics and quantum information processing. For example, the long-range and anisotropic character of dipolar interactions is predicted to enable the simulation of exotic spin-models (*7*) and the creation of novel states of matter (*8*, *9*). Additionally, molecular quantum states with robust coherence have been proposed as qubits in novel quantum computing platforms (*10*–*12*). Ideal qubits should experience strong interactions for gate operations but, during storage, interactions should be absent. Dipolar molecules may combine these two aspects in one physical system. An internal-state pair with long coherence time could act as a storage qubit, whereas long-range dipolar interactions between rotational qubits enable the processing of quantum information (*10*, *11*).

Dense, ultracold gases of diatomic molecules (*13*–*18*) provide ideal conditions for the study of coherence between internal molecular states. Ultracold molecular ensembles can be initialized in a single quantum state, and microwave fields can efficiently transfer molecular population between internal states (*19*–*21*). The coherence times between rotational states of ultracold $^{40}K^{87}Rb$ and $^{23}Na^{40}K$ molecules in the singlet vibrational ground state have been investigated and were found to be on the order of a few milliseconds (*20*, *22*). By localizing individual $^{40}K^{87}Rb$ molecules to the sites of an optical lattice, and with the help of spin-echo pulses, the rotational coherence time has been extended to tens of milliseconds (*23*). Although such coherence times were sufficiently long to spectroscopically reveal dipolar interactions between molecules, the interactions themselves serve as a source of decoherence for rotational states. So far, internal states with coherence times that are comparable to the lifetime of an ultracold molecular gas have remained elusive.

Here we report on the observation of second-scale coherence times between nuclear spin states of trapped ultracold fermionic $^{23}Na^{40}K$ molecules, which are a thousand times longer than the coherence times observed between rotational states under similar experimental conditions (*20*, *22*). The molecules are prepared in the singlet rovibrational ground state, where hyperfine levels correspond to pure nuclear spin degrees of freedom. We perform Ramsey spectroscopy on a pair of hyperfine levels and reveal their robust coherence. Multiple factors contribute to the robustness of the quantum superposition, starting with the insensitivity of the singlet rovibrational ground state to external fields. Specifically, we show that coherence is limited only by hertz-level light shifts that may further be eliminated via spin-echo techniques. We also demonstrate the absence of a density-dependent collisional shift. Such clock shifts, limiting the accuracy of Cs atomic clocks, are known to be suppressed in gases of identical fermions (*24*–*26*). Even for bosonic gases of singlet molecules, collisional interactions can be expected to be invariant under nuclear spin rotations. We therefore show that nuclear spin superpositions in

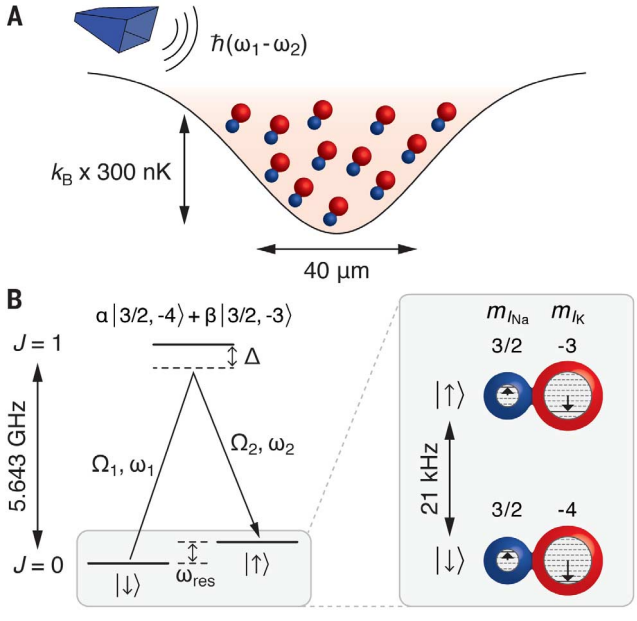

Fig. 1. Two-photon coupling between nuclear spin states of $^{23}Na^{40}K$ ground-state molecules. (**A**) The dense, ultracold ensemble is held in an optical dipole trap, and microwave fields are applied to coherently couple two nuclear spin states, $|\downarrow\rangle = |m_{I_{Na}} = 3/2, m_{I_K} = -4\rangle$ and $|\uparrow\rangle = |3/2, -3\rangle$, in the rotational ground state $J = 0$. $\hbar$, Planck's constant h divided by 2π; k_B, Boltzmann constant. (**B**) Level scheme of the two-photon microwave coupling. $\Omega_{1(2)}$ and $\omega_{1(2)}$ correspond to the Rabi coupling and microwave frequency, respectively, of the up-leg (down-leg) rotational transition. The ground and first excited rotational states $J = 0$ and $J = 1$ are separated by $h \times 5.643$ GHz. Δ denotes the single-photon detuning from the intermediate state, typically about $h \times 12$ kHz. The nuclear spins $|\downarrow\rangle$ and $|\uparrow\rangle$ are separated by about $h \times 21$ kHz. α and β denote the probability amplitudes of the respective spin contributions. The blue (red) spheres represent Na (K) atoms.

[1]Massachusetts Institute of Technology–Harvard Center for Ultracold Atoms, Research Laboratory of Electronics, Department of Physics, Massachusetts Institute of Technology, Cambridge, MA 02139, USA. [2]Center for Quantum Technologies, National University of Singapore, 3 Science Drive 2, Singapore 117543, Singapore.
*Present address: Department of Physics and Astronomy, Seoul National University, 1 Gwanak-ro, Gwanak-gu, Seoul 08826, Korea.
†Present address: Department of Physics, Columbia University, 538 West 120th Street, New York, NY 10027, USA.
‡Corresponding author. Email: zwierlein@mit.edu

molecules represent ideal candidates for storage qubits and time keepers in future precision measurements on dipolar quantum matter.

The experiment starts with the creation of $^{23}Na^{40}K$ molecules in the singlet rovibrational ground state $X^1\Sigma^+|v=0, J=0\rangle$ (*17*, *27*). Here, v denotes the vibrational quantum state, and J is the total angular momentum quantum number, neglecting nuclear spins. To reach the ground state, weakly bound Feshbach molecules of $^{23}Na^{40}K$ are created and subsequently transferred to the singlet rovibrational ground state by means of stimulated Raman adiabatic passage (STIRAP) (*17*, *28*). By choosing the polarization of the Raman beams appropriately, we create a pure ensemble of 2×10^3 ground-state molecules, all in the lowest energy hyperfine level. The molecular ensemble typically has an average density of $n = 2 \times 10^{10}$ cm^{-3} and a temperature of 300 nK and is trapped in a crossed optical dipole trap operating at a wavelength of $\lambda = 1064$ nm. Finally, the ground-state molecules are detected by a reverse STIRAP transfer back to Feshbach molecules and subsequent imaging of the ^{40}K component by using light resonant on the atomic cycling transition. This procedure selectively detects molecules in the lowest hyperfine level (*17*).

After the creation of ground-state molecules, a two-photon microwave pulse is applied to prepare each of the molecules in a superposition of two hyperfine levels within $|v=0, J=0\rangle$ (Fig. 1). At a magnetic field of 85.6 G, where the experiment operates, the 36 hyperfine levels in $J=0$ are split by the nuclear Zeeman effect (*17*, *20*). Hence, the nuclear spin projections $m_{I_{Na}}$ and m_{I_K} are good quantum numbers. The two levels that form the superposition state are the lowest hyperfine level $|m_{I_{Na}}, m_{I_K}\rangle = |3/2, -4\rangle$ and the first excited hyperfine level $|3/2, -3\rangle$, denoted by $|\downarrow\rangle$ and $|\uparrow\rangle$, respectively. For the coherent transfer between $|\downarrow\rangle$ and $|\uparrow\rangle$, a hyperfine level with mixed $m_{I_K} = -4$ and -3 character in the rotationally excited $|v=0, J=1\rangle$ state (*20*) is used as an intermediate state to drive two-photon Rabi oscillations (*27*).

Ramsey precession is initiated by applying a $\pi/2$-pulse near the microwave two-photon resonance. Subsequently, the superposition state undergoes field-free time evolution with respect to the unperturbed resonance frequency ω_{res}. After a hold time T, we apply a second $\pi/2$-pulse and record the number of molecules in $|\downarrow\rangle$ (Fig. 2). By fitting the observed Ramsey precession with a model that incorporates the decay of molecule number and coherence (*27*), we extract the molecule lifetime T_1 and the coherence time T_2^*. At a molecular lifetime of $T_1 = 1.9(5)$ s, we observe a coherence time on the scale of a second, $T_2^* = 0.7(3)$ s, which is a thousand times longer than rotational coherence times measured similarly without spin-echo techniques. The oscillation frequency of the Ramsey precession is given by the difference of the two-photon microwave drive, $\omega_1 - \omega_2$, and the unperturbed resonance frequency, ω_{res}. From this, we extract the energy difference between $|\downarrow\rangle$ and $|\uparrow\rangle$ to be $\omega_{res} = 2\pi \times 20.514(10)$ kHz at a magnetic field of 85.6 G, which allows us to

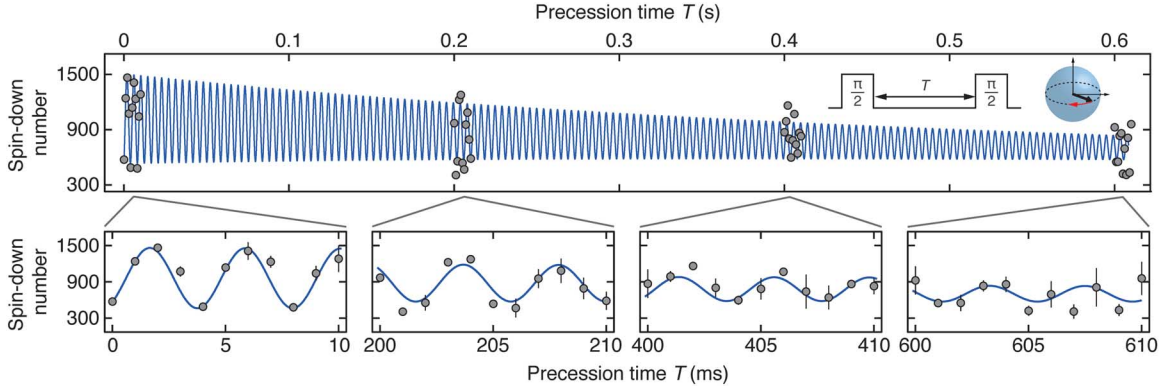

Fig. 2. Coherent Ramsey precession of nuclear spin states in $^{23}Na^{40}K$. An initial $\pi/2$-pulse, resonant on the dressed two-photon transition, creates a superposition of the $|\downarrow\rangle$ and $|\uparrow\rangle$ states in the equatorial plane of the Bloch sphere (see inset). The Bloch vector precesses at a frequency $|(\omega_1 - \omega_2) - \omega_{res}|$ for a variable precession time T until a second resonant $\pi/2$-pulse completes the Ramsey sequence. The solid blue line is a fit of the complete data set with a single oscillation frequency and phase (*27*), indicating the phase coherence of the Ramsey precession. The bottom row shows magnified sections of the full data set above. Data points correspond to the average of typically three experimental runs; the error bars denote the standard deviation of the mean.

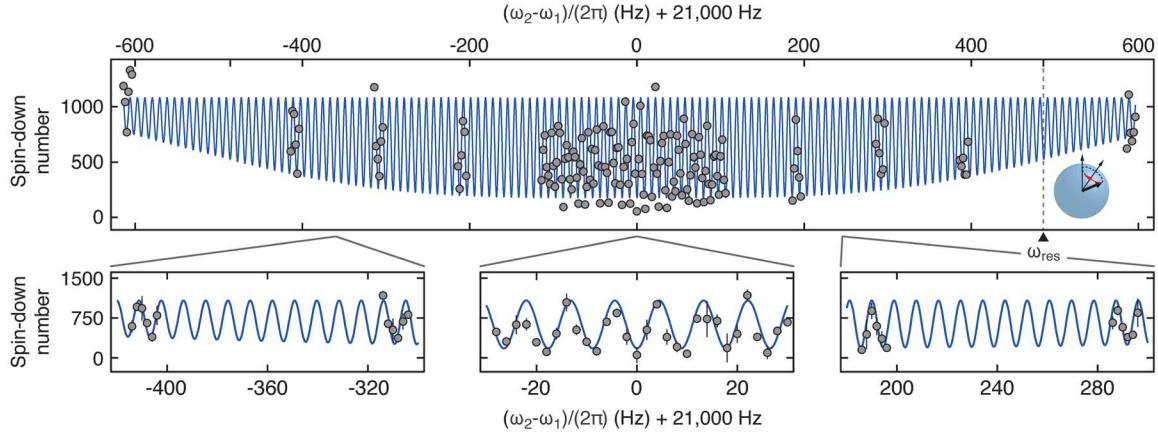

Fig. 3. High-resolution Ramsey spectroscopy. Ramsey fringes are recorded as a function of two-photon drive frequency $\omega_1 - \omega_2$, keeping the precession time $T = 112$ ms fixed. The distance between adjacent Ramsey fringes is $1/T \approx 8.9$ Hz, resulting in hertz-level precision. The solid blue line shows a fit with a Ramsey line shape function that includes, as a free parameter, the two-photon Rabi coupling Ω (*27*), which determines the overall envelope of the spectrum.

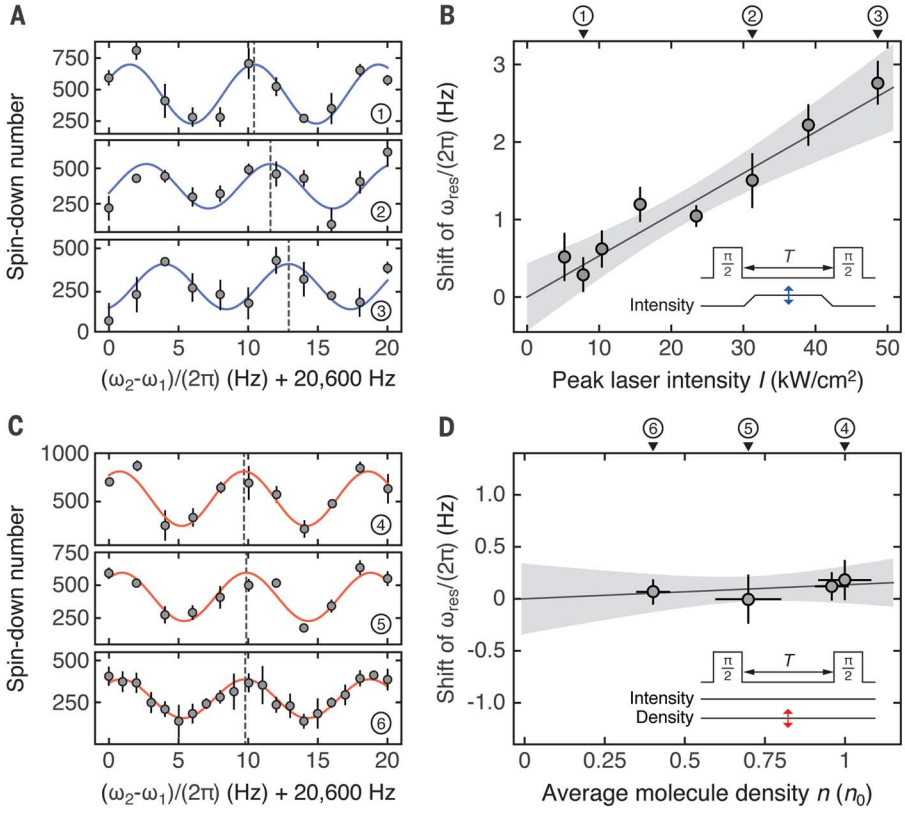

Fig. 4. Hertz-level light shifts and absence of density-dependent clock shift. A shift in the Ramsey fringes corresponds to a change in the resonance frequency between $|\downarrow\rangle$ and $|\uparrow\rangle$. (**A**) Ramsey spectroscopy for various dipole trap laser intensities. The intensity of the trap laser is adiabatically varied in the first and the final 20 ms of the free precession time T = 112 ms [inset of (B)]. The solid lines show sine fits, which are used to extract the phase of the Ramsey fringes. For the fits, the oscillation frequency is set by the precession time, and only the phase and the amplitude of the oscillations are taken as free parameters. (**B**) Shift of the resonance frequency as a function of peak dipole trap–laser intensity. A linear fit (solid line) yields a slope of 50(10) mHz/(kW/cm^2); the gray-shaded area reflects the 95% confidence interval of the fit. (**C**) Ramsey spectroscopy for various molecule densities at a constant trap-laser intensity of 31 kW/cm^2. The average densities are normalized with respect to $n_0 = 2.5 \times 10^{10}$ cm^{-3}. Solid lines show sine fits. (**D**) Shift of the resonance frequency as a function of molecular density. The gray-shaded area reflects the 95% confidence interval of a linear fit. The fit is consistent with the absence of a collisional shift. Data points in (A) and (C) correspond to the average of two experimental runs, and error bars denote the standard deviation of the mean.

precisely determine the weak nuclear spin–spin coupling constant of ^{23}Na^{40}K as $c_4 = -409(10)$ Hz.

Utilizing the long coherence time between $|\downarrow\rangle$ and $|\uparrow\rangle$, we record a high-resolution Ramsey fringe (Fig. 3). The spectrum is measured by varying the microwave drive frequency, $\omega_1 - \omega_2$, while keeping the precession time T between the $\pi/2$-pulses constant. The spacing between the Ramsey fringes is given by $2\pi/T$. Systematic sources of energy shifts between $|\downarrow\rangle$ and $|\uparrow\rangle$ can be varied during the free precession time, and a differential measurement of the Ramsey phase shift reveals these effects with hertz precision. The afforded spectral resolution can be compared to typical dipolar-interaction energies $E_d = nd^2/(4\pi\varepsilon_0)$, where d is the induced dipole moment and ε_0 is the vacuum permittivity. For molecular densities achieved in this work, E_d can reach tens of hertz. Ramsey spectroscopy on nuclear spin states can thus serve as a highly sensitive probe for dipolar interactions, allowing the characterization of many-body quantum states (*23, 29*).

The observed long coherence times result from the favorable properties of the singlet rovibrational ground state and the Fermi statistics of ^{23}Na^{40}K. As the molecules are in the $J = 0$ state of $X^1\Sigma^+$, the rotational angular momentum, the electronic spin, and the projection of the orbital angular momentum along the internuclear axis all vanish. Therefore, the electronic wave function is fully decoupled from the nuclear spins, and the ac-polarizability is, to a high degree, identical for all $J = 0$ nuclear spin states. This leads to a suppression of light-induced dephasing present in a nonuniform optical potential. Also, dephasing induced by magnetic field fluctuations is reduced because the only internal degrees of freedom that couple to external magnetic fields are the nuclear spins, whose magnetic moments are $m_e/m_n \sim 1/2000$ smaller compared to that of an electronic spin. Finally, the absence of s-wave collisions between identical fermionic ^{23}Na^{40}K molecules and the suppression of p-wave collisions at ultracold temperatures reduce collisional dephasing (*24, 25*). Even without Pauli blocking, for singlet molecules in $J = 0$, one may expect a near-perfect invariance of collisional interactions under nuclear spin rotations.

To explore the limitations of coherence, we use Ramsey spectroscopy to precisely measure the variation in energy splitting between $|\downarrow\rangle$ and $|\uparrow\rangle$ as a function of trap-laser intensity and molecular density. Changes in the resonance will appear as a phase shift of the Ramsey fringes, recorded for a fixed precession time T. First, the effect of the trapping light is investigated by varying the dipole trap–laser intensity that the molecules experience during free precession time. This is done by adiabatically ramping the trap-laser intensity from an initial value of 7.5 kW/cm^2 to a final value between 5 and 50 kW/cm^2 after the first $\pi/2$-pulse, and back to the initial value before the second $\pi/2$-pulse (Fig. 4B, inset). The corresponding Ramsey spectra are shown in Fig. 4, A and B. The resonance frequency increases with laser intensity, shifting by up to 3 Hz within the investigated range. However, when the laser intensity is varied, both the average density and the temperature of the molecular cloud are changed. For the explored range of intensities, the average density varies between 0.9×10^{10} and 3.5×10^{10} cm^{-3} and the temperature varies between 300 and 750 nK. To distinguish a light-induced ac-Stark shift from a density-dependent collisional shift, we perform Ramsey spectroscopy for varying density but constant light intensity (Fig. 4, C and D). We explore average molecular densities between $n = 1.0 \times 10^{10}$ cm^{-3} and 2.5×10^{10} cm^{-3}, keeping the trap-laser intensity fixed at 31 kW/cm^2. The temperature of the molecular ensembles is kept constant at 600 nK. For the highest density (Fig. 4D), the resonance shift can be constrained to 130(180) mHz, consistent with the absence of a collisional shift. From this, we infer that the resonance shift in Fig. 4B dominantly originates from a light-induced ac-Stark shift that likely arises from spin-orbit coupling and induced hyperfine structure in the electronically excited molecular states (*17*). Because the trap-laser intensity varies across the molecular cloud, a light-induced shift of ω_{res} leads to a dephasing of the superposition state following the first $\pi/2$-pulse. Indeed, a direct measurement of the coherence time versus laser intensity reveals a monotonic decrease of coherence, consistent with the measured differential ac-Stark shift (*27*). This implies that coherence times of molecular qubits can be further improved by using uniform trapping potentials (*30*), which could largely eliminate the impact of ac-Stark shifts. For isolated molecules, coherent control sequences, such as spin-echo, may further prolong the coherence time. The eventual coherence limit for bulk gases will be the trap lifetime, on the order of several seconds for our chemically stable NaK molecules (*17*). This lifetime may

be limited by inelastic collisions, possibly enhanced by the formation of long-lived molecular complexes (*31*), or by trapping light-induced collisions. Collisions between ultracold molecules, both elastic and inelastic, are currently a topic of strong interest (*32*), and future insights may lead to a substantial increase in the lifetimes of dense molecular gases.

Our observation of second-scale coherence times in trapped $^{23}Na^{40}K$ molecules provides strong support for the use of molecules as a versatile quantum resource for quantum information (*10*). Confined in optical lattices under quantum-gas microscopes (*33*, *34*), in optical microtraps (*35*), or in ion traps (*36*), it will be possible to individually address, control, and detect internal states of single molecules. Coherent manipulation of molecular rotational states with microwave radiation allows full control of long-range dipolar interactions, which should enable gate operations between pairs of molecules (*11*). This work also suggests routes for precision metrology with ultracold molecules. Transitions between nuclear spin states of different vibrational states may exhibit similarly long coherence times, enabling hertz-level molecular spectroscopy in the optical domain and bringing optical molecular clocks into experimental reach (*37*–*39*).

REFERENCES AND NOTES

1. S. Haroche, J. M. Raimond, *Exploring the Quantum* (Oxford Univ. Press, 2006).
2. L. D. Carr, D. DeMille, R. V. Krems, J. Ye, *New J. Phys.* **11**, 055049 (2009).
3. R. Krems, B. Friedrich, W. C. Stwalley, Eds., *Cold Molecules: Theory, Experiment, Applications* (CRC Press, 2009).
4. T. Zelevinsky, S. Kotochigova, J. Ye, *Phys. Rev. Lett.* **100**, 043201 (2008).
5. D. DeMille *et al.*, *Phys. Rev. Lett.* **100**, 043202 (2008).
6. J. Baron *et al.*, *Science* **343**, 269–272 (2014).
7. A. Micheli, G. K. Brennen, P. Zoller, *Nat. Phys.* **2**, 341–347 (2006).
8. N. R. Cooper, G. V. Shlyapnikov, *Phys. Rev. Lett.* **103**, 155302 (2009).
9. H. P. Büchler *et al.*, *Phys. Rev. Lett.* **98**, 060404 (2007).
10. D. DeMille, *Phys. Rev. Lett.* **88**, 067901 (2002).
11. S. F. Yelin, K. Kirby, R. Cote, *Phys. Rev. A* **74**, 050301 (2006).
12. A. André *et al.*, *Nat. Phys.* **2**, 636–642 (2006).
13. J. G. Danzl *et al.*, *Science* **321**, 1062–1066 (2008).
14. K. K. Ni *et al.*, *Science* **322**, 231–235 (2008).
15. T. Takekoshi *et al.*, *Phys. Rev. Lett.* **113**, 205301 (2014).
16. P. K. Molony *et al.*, *Phys. Rev. Lett.* **113**, 255301 (2014).
17. J. W. Park, S. A. Will, M. W. Zwierlein, *Phys. Rev. Lett.* **114**, 205302 (2015).
18. M. Guo *et al.*, *Phys. Rev. Lett.* **116**, 205303 (2016).
19. S. Ospelkaus *et al.*, *Phys. Rev. Lett.* **104**, 030402 (2010).
20. S. A. Will, J. W. Park, Z. Z. Yan, H. Loh, M. W. Zwierlein, *Phys. Rev. Lett.* **116**, 225306 (2016).
21. P. D. Gregory, J. Aldegunde, J. M. Hutson, S. L. Cornish, *Phys. Rev. A* **94**, 041403 (2016).
22. B. Neyenhuis *et al.*, *Phys. Rev. Lett.* **109**, 230403 (2012).
23. B. Yan *et al.*, *Nature* **501**, 521–525 (2013).
24. S. Gupta *et al.*, *Science* **300**, 1723–1726 (2003).
25. M. W. Zwierlein, Z. Hadzibabic, S. Gupta, W. Ketterle, *Phys. Rev. Lett.* **91**, 250404 (2003).
26. A. D. Ludlow, M. M. Boyd, J. Ye, E. Peik, P. O. Schmidt, *Rev. Mod. Phys.* **87**, 637–701 (2015).
27. See supplementary materials.
28. J. W. Park, S. A. Will, M. W. Zwierlein, *New J. Phys.* **17**, 075016 (2015).
29. K. R. A. Hazzard, A. V. Gorshkov, A. M. Rey, *Phys. Rev. A* **84**, 033608 (2011).
30. A. L. Gaunt, T. F. Schmidutz, I. Gotlibovych, R. P. Smith, Z. Hadzibabic, *Phys. Rev. Lett.* **110**, 200406 (2013).
31. M. Mayle, G. Quéméner, B. P. Ruzic, J. L. Bohn, *Phys. Rev. A* **87**, 012709 (2013).
32. G. Quéméner, P. S. Julienne, *Chem. Rev.* **112**, 4949–5011 (2012).
33. W. S. Bakr, J. I. Gillen, A. Peng, S. Fölling, M. Greiner, *Nature* **462**, 74–77 (2009).
34. J. F. Sherson *et al.*, *Nature* **467**, 68–72 (2010).
35. A. M. Kaufman, B. J. Lester, C. A. Regal, *Phys. Rev. X* **2**, 041014 (2012).
36. H. Loh *et al.*, *Science* **342**, 1220–1222 (2013).
37. S. Schiller, D. Bakalov, V. I. Korobov, *Phys. Rev. Lett.* **113**, 023004 (2014).
38. J.-P. Karr, *J. Mol. Spectrosc.* **300**, 37–43 (2014).
39. C. Cheng *et al.*, *Phys. Rev. Lett.* **117**, 253201 (2016).

ACKNOWLEDGMENTS

We thank R. Field and collaborators, K.-K. Ni, and T. Nicholson for fruitful discussions. This work was supported by the NSF, the Air Force Office of Scientific Research (AFOSR) Presidential Early Career Award for Scientists and Engineers, the U.S. Army Research Office (ARO), an ARO Multidisciplinary University Research Initiative (MURI) on "High-Resolution Quantum Control of Chemical Reactions," an AFOSR MURI on "Exotic Phases of Matter," and the David and Lucile Packard Foundation. Z.Z.Y. acknowledges additional support from the NSF Graduate Research Fellowship Program. The data supporting this manuscript are available from the corresponding author on request.

SUPPLEMENTARY MATERIALS

www.sciencemag.org/content/357/6349/372/suppl/DC1
Materials and Methods
Figs. S1 and S2
References (*40*–*43*)

1 December 2016; accepted 23 June 2017
10.1126/science.aal5066

Second-scale nuclear spin coherence time of ultracold $^{23}Na^{40}K$ molecules

Jee Woo Park, Zoe Z. Yan, Huanqian Loh, Sebastian A. Will and Martin W. Zwierlein

Science **357** (6349), 372-375.
DOI: 10.1126/science.aal5066

Extending the coherence time of molecules

Quantum properties of atoms and molecules can be exploited for precision measurements or quantum information processing. The complex state structure of molecules can be exploited, but it is hard to preserve the coherence between pairs of those states in applications. Park *et al.* created fermionic molecules of NaK in the rovibrational ground state that maintained coherence between their nuclear spin states on a time scale of 1 second. This long coherence time makes dipolar ultracold molecules a valuable quantum resource.

Science, this issue p. 372